

Identification of a Novel Selective Serotonin Reuptake Inhibitor by Coupling Monoamine Transporter-Based Virtual Screening and Rational Molecular Hybridization

Tammy L. Nolan,^{†,‡} David J. Lapinsky,^{*†} Jeffery N. Talbot,[§] Martín Indarte,^{||} Yi Liu,[†] Sankar Manepalli,[‡] Laura M. Geffert,[†] Mary Ellen Amos,[§] Phillip N. Taylor,[§] Jeffry D. Madura,^{*‡} and Christopher K. Surratt^{*†}

[†]Division of Pharmaceutical Sciences, Mylan School of Pharmacy, Duquesne University, 600 Forbes Avenue, Pittsburgh, Pennsylvania 15282, United States

[‡]Departments of Chemistry and Biochemistry, Center for Computational Sciences, Duquesne University, 600 Forbes Avenue, Pittsburgh, Pennsylvania 15282, United States

[§]Department of Pharmaceutical and Biomedical Sciences, Raabe College of Pharmacy, Ohio Northern University, 525 South Main Street, Ada, Ohio 45810, United States

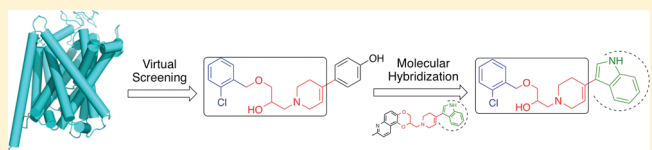
^{||}Institute of Biotechnology and Biomedicine, Universitat Autònoma de Barcelona, 08193 Bellaterra, Spain

 Supporting Information

ABSTRACT: Ligand virtual screening (VS) using the vestibular binding pocket of a three-dimensional (3-D) monoamine transporter (MAT) computational model followed by in vitro pharmacology led to the identification of a human serotonin transporter (hSERT) inhibitor with modest affinity (hSERT $K_i = 284$ nM). Structural comparison of this VS-elucidated

compound, denoted MI-17, to known SERT ligands led to the rational design and synthesis of DJLDU-3-79, a molecular hybrid of MI-17 and dual SERT/5-HT_{1A} receptor antagonist SSA-426. Relative to MI-17, DJLDU-3-79 displayed 7-fold improvement in hSERT binding affinity and a 3-fold increase in [³H]-serotonin uptake inhibition potency at hSERT-HEK cells. This hybrid compound displayed a hSERT:hDAT selectivity ratio of 50:1 and a hSERT:hNET (human norepinephrine transporter) ratio of >200:1. In mice, DJLDU-3-79 decreased immobility in the tail suspension test comparable to the SSRI fluvoxamine, suggesting that DJLDU-3-79 may possess antidepressant properties. This proof of concept study highlights MAT virtual screening as a powerful tool for identifying novel inhibitor chemotypes and chemical fragments for rational inhibitor design.

KEYWORDS: monoamine, neurotransmitter transporter, virtual screening, molecular docking, molecular hybridization, depression



The plasma membrane monoamine transporter (MAT) proteins (the dopamine transporter (DAT), serotonin transporter (SERT), and norepinephrine transporter (NET)) are relevant to central nervous system (CNS)-based maladies including substance abuse and addiction,¹ orthostatic hypotension,² attention-deficit hyperactivity disorder (ADHD),³ Lesch-Nyhan disease,⁴ autism,⁵ depression,^{6,7} and obsessive-compulsive and other anxiety disorders.⁸ MATs represent pivotal targets for readily recognized medications such as methylphenidate (Ritalin), fluoxetine (Prozac), and amitriptyline (Elavil). The development of drugs targeting MATs has been via traditional ligand-based (usually substrate analogue) approaches. Few chemical scaffolds have been identified; this shortcoming provides motivation to develop new tools that enable the discovery of structurally novel lead compounds. The present work illustrates the rational transformation of a DAT virtual screening (VS) hit ligand to a serotonin-selective reuptake inhibitor (SSRI) through a molecular hybridization approach.

With respect to the armamentarium of antidepressant drugs, another SSRI therapeutic may appear to be unnecessary; however, SSRI drugs currently on the market are characterized by inefficacy in

many patients and whose use is often limited by adverse effects. As examples, citalopram (Celexa) is associated with insomnia, paroxetine (Paxil) is well-known for somnolence and weight gain, sertraline (Zoloft) is especially problematic in causing gastrointestinal disturbances, and fluvoxamine (Luvox) has been associated with dangerous drug interactions. All SSRIs have been linked to sexual dysfunction.^{9–12} The adverse effects of these drugs are generally linked to secondary interactions with one or more of the 14 types of serotonin receptors. Development of an SSRI structurally dissimilar to those currently available could reduce the likelihood of undesirable interactions with these receptors.

The DAT, SERT, and NET are primarily responsible for the respective clearance of dopamine, serotonin, and norepinephrine from the synaptic cleft. A sodium gradient is used to power neurotransmitter uptake by these MATs back into the presynaptic neuron, terminating stimulation of postsynaptic receptors.

Received: May 5, 2011

Accepted: June 8, 2011

Published: June 08, 2011

One MAT substrate molecule, a Cl^- ion, and either one or two Na^+ ions are transported across the plasma membrane through a symport method. The SERT additionally requires antiport movement of one K^+ ion.^{13–15} The MATs are members of the neurotransmitter/sodium symporter (NSS) family, which includes bacterial and eukaryotic transporters. NSS proteins share 20–30% sequence identity¹⁶ and are characterized by 12 transmembrane domains (TM) and intracellular N- and C-termini. Crystallization of the leucine transporter LeuT,¹⁷ a bacterial NSS member, has provided a template for generation of three-dimensional (3-D) MAT computer models for use in structure–function studies. LeuT-based MAT homology models have proven useful in guiding site-directed mutagenesis, studies on substrate translocation mechanism, and elucidation of ligand binding sites.^{18–21}

Two discrete ligand binding sites within the MAT proteins have been established. The primary substrate site, S1, is at the approximate midpoint of the lipid bilayer and is flanked by gating residues that alternate access between the intracellular and extracellular regions.^{17,19,22,23} A second substrate site, S2, is to the extracellular side of the external gate of S1, in what is termed the extracellular vestibule.^{20,22,24,25} The substrate occupies S2 before its translocation to the interior S1 site.^{24,25} MAT inhibitors have been associated with the S1^{22,26,27} and S2^{21,28–30} sites and, apparently, the region between the sites.³¹ SSRIs and psychostimulants are most often associated with the S1 site and the tricyclic antidepressants with the S2 site or general vestibular region, but exceptions have been reported.^{26,30}

To date, no LeuT protein-inhibitor ligand cocrystal structures have been obtained in which the inhibitor occupies the S1 site, adding to the difficulty in modeling MAT–inhibitor interactions. Consequently, de novo, unbiased docking of inhibitors to MAT computational models of the type utilized in ligand VS is currently limited to the extracellular vestibule. Screening of thousands to millions of potential ligands in a structural library using a receptor molecular model is a powerful, rapid, and inexpensive tool for discovery of lead compounds.^{32,33} Recently, the vestibular pocket of a MAT computational model was employed for VS of a chemical library, identifying novel inhibitor chemotypes.³⁴ The work described herein couples the VS process with traditional medicinal chemistry drug design to yield a novel SSRI.

RESULTS AND DISCUSSION

The vestibular binding pocket of a previously described LeuT-based rDAT homology model³⁴ was used for VS of the entire ENAMINE virtual screening collection, a database containing approximately 3 million compounds. Utilizing MOE (Molecular Operating Environment) Affinity dG scoring³⁵ and visual inspection that focused on optimizing intramolecular interactions, 10 compounds from the database were selected and purchased for initial hMAT pharmacological evaluation. These VS “hits” (Figure A in the Supporting Information) were tested at 10 μM final concentration in one-point binding inhibition assays that displaced the radiolabeled cocaine analogues [^3H]-WIN 35,428 (hDAT) or [^{125}I]-RTI-55 (hSERT, hNET). Three of the 10 VS compounds, coded MI-15, MI-17, and MI-20, displayed significant radioligand binding inhibition of 40% or more at all three MATs (Figure 1). Tetrahydropyridinyl compound MI-17 ((\pm)-1, Figure 2) was the most potent MAT inhibitor in the screening assay and was more thoroughly characterized.

MI-17 affinity at hSERT, measured by displacement of radiolabeled cocaine analogue, was a modest 284 nM; the hSERT

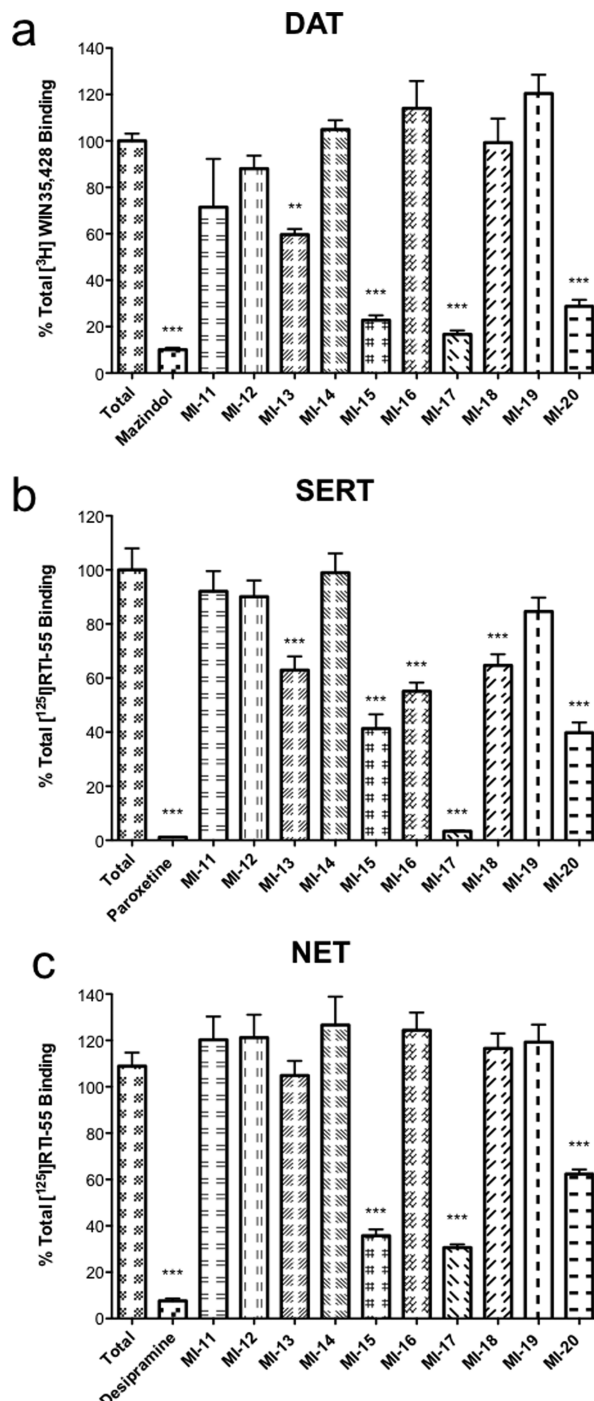


Figure 1. Pharmacological one-point ($10 \mu\text{M}$) binding assay of virtual screening hits at (A) hDAT-N2A using [^3H]-WIN 35,428 and mazindol ($10 \mu\text{M}$) for nonspecific binding, (B) hSERT-HEK293 using [^{125}I]-RTI-55 and paroxetine ($10 \mu\text{M}$) for nonspecific binding, and (C) hNET-HEK293 using [^{125}I]-RTI-55 and desipramine ($10 \mu\text{M}$) for nonspecific binding. Data represent $n = 3$ independent experiments. ** $P < 0.002$ vs total binding in that assay; *** $P < 0.0001$ vs total binding in that assay.

affinity was 4.6-fold higher than that for hDAT and 19-fold higher than that for hNET (Table 1). The potency of MI-17 in inhibiting uptake of cognate [^3H]-neurotransmitter was over 3-fold higher at hSERT than at hDAT and hNET. Given the sequence similarity among the three hMATs, the discovery of a

modest hSERT ligand by VS using a DAT homology model was not surprising. Interestingly, SciFinder Scholar reveals no primary literature associated with MI-17 ((\pm)-1); rather, it is simply available in milligram quantities from limited chemical sources. A literature survey of known SERT inhibitors³⁶ indicated that SSA-426 (2, Figure 2), a Wyeth Pharmaceuticals dual SERT/5-HT_{1A} receptor antagonist, has high affinity for rat SERT ($K_i = 2.34 \pm 0.59$ nM).³⁷ The tetrahydropyridine indole portion of 2 appears to be important for SERT binding, as several high-affinity SERT ligands containing this chemical signature have been reported.^{38–40}

Apart from the conserved tetrahydropyridine ring and 2,3-dioxypropyl N-substituent (boxed regions of Figure 2), compounds 1 and 2 appear structurally dissimilar. However, flexible alignment illuminated their chemical similarities and a common 3-D arrangement of certain structural features (Figure 3a). In the top-scoring low energy conformation alignment, the tetrahydropyridine moieties were aligned as were the phenol and indole rings, while the alcohol and ether oxygen atoms of 1 overlapped the dioxane ether oxygen atoms of 2. Additional docking studies were carried out to further explore the possible ligand-binding conformations of these compounds within hSERT (Figure 3b). In agreement with alignment studies, the top-scoring poses suggested that (\pm)-1 and 2 occupy the vestibular pocket in similar orientations. In particular, the phenol of (*R*)-1 and the indole of 2 docked deep in the vestibular pocket, essentially in the S2 substrate site,^{20,24} while the variable tetrahydropyridine *N*-substituents were accessible to the extracellular environment (Figure 3c and d).

Taking into account the suggested binding modes and common structural motifs for (\pm)-1 and 2, and the established importance of indoles in SERT recognition,³⁶ DJLDU-3-79 ((\pm)-3) was rationally designed as a molecular hybrid⁴¹ of MI-17 ((\pm)-1) and SSA-426 (2) (Figure 2). The hypothesis was that replacing the phenol in (\pm)-1 with the indole in 2 would improve hSERT selectivity and affinity. The synthesis of hybrid compound (\pm)-3 is depicted in Scheme 1.

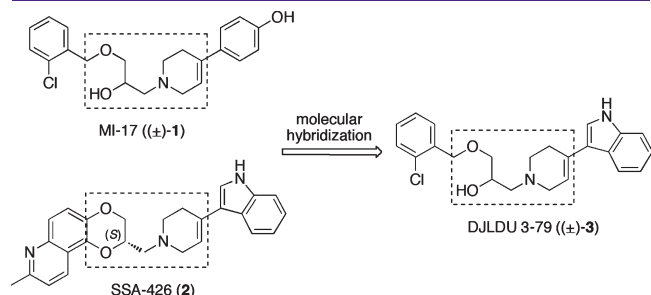


Figure 2. Structural comparison of virtual screening hit MI-17 ((\pm)-1) with dual SERT/5HT_{1A} receptor antagonist SSA-426 (2), leading to the rational design of DJLDU-3-79 ((\pm)-3) via molecular hybridization.

Table 1. MI-17 ((\pm)-1) and DJLDU-3-79 ((\pm)-3) Apparent hMAT Binding Affinities and Neurotransmitter Uptake Inhibition Potencies^a

	binding affinity (K_b , nM)			selectivity ratio		substrate uptake inhibition potency (IC_{50} , nM)		
	DAT ^b	SERT ^c	NET ^d	SERT/DAT	SERT/NET	DAT ^b	SERT ^c	NET ^d
(\pm)-1	1298 \pm 36	284 \pm 66 ^e	5300 \pm 1341	4.6	19	3774 \pm 407	1167 \pm 26 ^e	3764 \pm 446
(\pm)-3	2129 \pm 177	37 \pm 4 ^{e,f}	>10 000	50	>200	3436 \pm 245	441 \pm 62 ^e	>10 000

^a Values are mean \pm standard error for 3–5 independent experiments, each performed in duplicate. Stably transfected hDAT-N2A, hSERT-HEK293, and hNET-HEK293 cells were used. ^b K_b determined using [³H]-WIN 35,428; IC_{50} determined using [³H]-dopamine. ^c K_b determined using [¹²⁵I]-RTI-55; IC_{50} determined using [³H]-serotonin. ^d K_b determined using [¹²⁵I]-RTI-55; IC_{50} determined using [³H]-norepinephrine. ^e $P < 0.05$ for hSERT vs hDAT in the same assay. ^f $P < 0.05$ for (\pm)-1 vs (\pm)-3 in the binding assay.

Briefly, epoxide (\pm)-4 was prepared in 97% yield by benzylating racemic epichlorohydrin with 2-chlorobenzyl alcohol analogous to that described by Sun et al.⁴² The epoxide was then opened with 3-(1,2,3,6-tetrahydropyridin-4-yl)-1*H*-indole (5)⁴³ similar to that described by Chan et al.⁴⁴ to provide target (\pm)-3 in good yield (95%). Pharmacological evaluation of (\pm)-3 validated the rational attempt to modify VS hit compound MI-17 to improve hSERT selectivity, binding affinity, and substrate uptake inhibition potency (Table 1). While only a 1.6-fold decrease in hDAT binding affinity was observed for (\pm)-3 relative to lead compound (\pm)-1, hSERT affinity increased 6.8-fold with the same modification. Thus, hSERT selectivity over hDAT increased from 4.6-fold to 50-fold. Additionally, inhibition of [¹²⁵I]-RTI-55 binding and [³H]-norepinephrine uptake at hNET were undetectable for (\pm)-3 (K_b and IC_{50} values $> 10 \mu\text{M}$), rendering an hSERT to hNET selectivity of over 200-fold.

The in vitro SERT-selective properties of DJLDU-3-79 ((\pm)-3) were next tested for translatability to an in vivo model. The tail suspension test (TST) is a well-established prototypical rodent model of learned helplessness^{45,46} that is strongly correlated to drugs that possess antidepressant-like activity in humans. This assay is based in part on findings that drugs that possess antidepressant activity in humans reduce the immobility time of the animal in this test. Because of their in vitro characteristics analogous to therapeutically relevant antidepressants that block uptake of monoamine neurotransmitters involved in the regulation of mood, (\pm)-1 and (\pm)-3 were screened in mice for antidepressant-like effects in the TST.

Mice treated with (\pm)-3 produced a dose-dependent decrease in immobility time in the TST that was comparable in effect to the SSRI fluvoxamine and the norepinephrine selective reuptake inhibitor desipramine (Figure 4). Compound (\pm)-3 did not alter general locomotor behavior (Figure 5A). These data suggest that (\pm)-3 could have potent and efficacious antidepressant-like activity. In contrast, (\pm)-1 dose-dependently increased immobility times in the TST in two different preparations: 2% DMSO vehicle (Figure 4C) or 55% DMSO vehicle in the oxalate form (data not shown). Unlike (\pm)-3, (\pm)-1 significantly altered spontaneous activity and gross behaviors (Figure 5B), particularly at doses greater than 3 mg/kg, which potentially accounts for increased immobility observed in the TST. Thus, (\pm)-1 has potentially debilitating effects on animal activity and gross behavior such that its use in behavioral-based paradigms may be contraindicated.

To date, there has been only one report of a MAT model-based VS effort that yielded active compounds,³⁴ in part due to the complexity of obtaining discrete transporter conformations at high resolution. Even reports of ligand-based VS approaches are few.^{47,48} Considering that MAT inhibitors serve to increase synaptic levels of monoamine neurotransmitter, modulation of

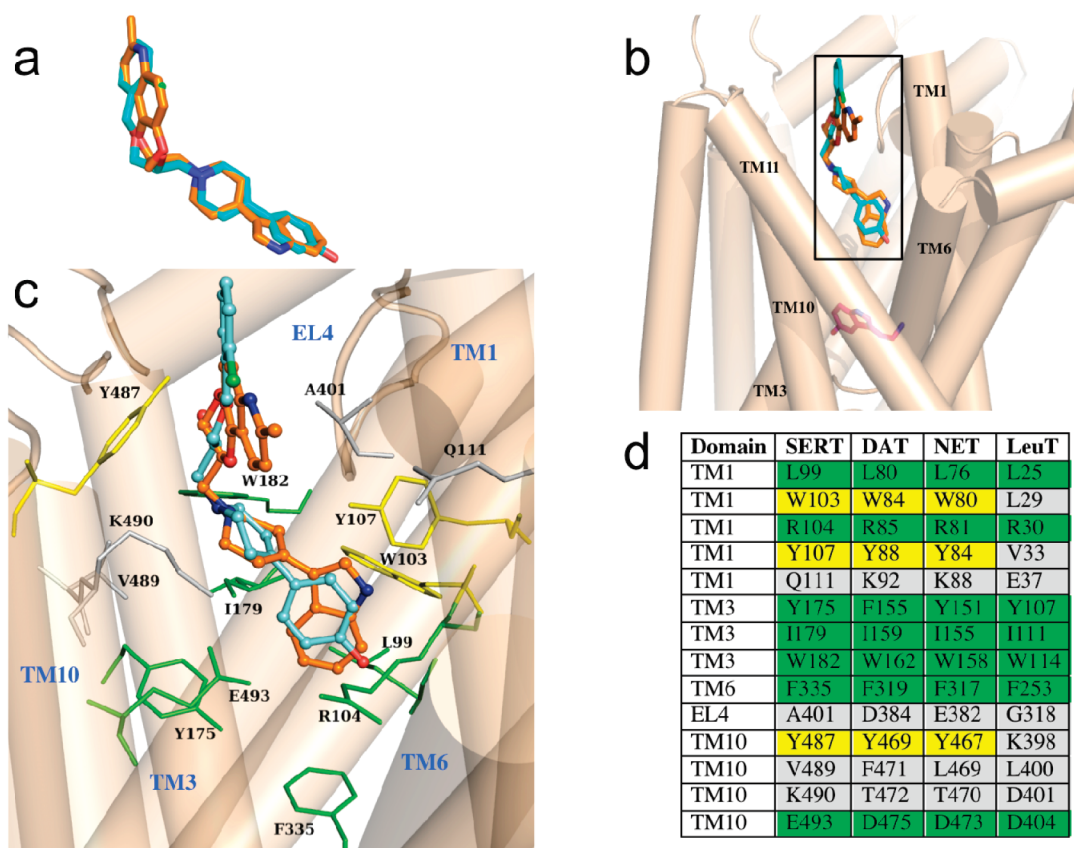
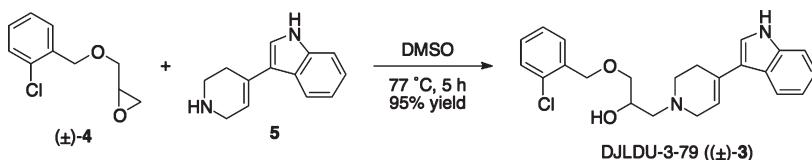


Figure 3. (a) Flexible alignment showing the similar 3-D arrangement for low-energy conformations of (\pm)-1 (cyan, R-enantiomer pictured) and 2 (orange). (b) High-scoring docking poses of (\pm)-1 (cyan, R-enantiomer pictured) and 2 (orange) in the vestibular S2 binding site of hSERT (beige cylinders) are superposed; the S1 substrate pocket is defined by a serotonin molecule (magenta). (c) Residues predicted for the hSERT vestibular S2 pocket. Residues within 4.5 Å of (+)-1 (cyan) and 2 (orange) are pictured. The color code indicates residues identical among the MATs and LeuT (green), residues shared among only the MATs (yellow), and nonidentical residues (gray). TM 11 was removed in this panel to facilitate viewing of the relevant side chains. (d) Comparison of predicted S2 pocket residues among hSERT, hDAT, hNET, and LeuT. Colors correspond to panel (c). The local sequence identities for hSERT are 23% between hSERT and LeuT, 38% between hSERT and hDAT, and 42% between hSERT and hNET. Figures were generated using PyMOL.⁶³

Scheme 1. Synthesis of MI-17/SSA-426 Hybrid Compound DJLDU-3-79 ((\pm)-3)



postsynaptic monoamine receptors is another therapeutic avenue. Starting with rhodopsin, findings from two decades of high resolution structure–function studies of the G protein coupled receptors (GPCRs) are available.⁴⁹ Just as crystallization of LeuT launched credible MAT computational modeling, the success in obtaining X-ray structures of the β_1 and β_2 adrenergic receptors^{50,51} and a dopamine D3 receptor–antagonist drug cocrystal⁵² has stimulated especially reliable model building of the monoamine GPCRs and their subsequent use as VS tools. Novel 5-HT_{2A} and 5-HT_{2C} ligands have been identified via VS, with the latter including compounds with low nanomolar affinity.^{53–55} Active conformations of adrenergic and serotonergic GPCRs have been modeled using molecular dynamics followed by

validation using VS of a structural database enriched with classic ligands for each receptor.^{54,56} In a unique and intriguing approach, molecular models based on the adrenergic receptor crystal structures have been used to map potentially druggable allosteric pockets of the receptor.⁵⁷ As more is elucidated connecting specific monoamine receptor subtypes to depression and other CNS disease states, it is anticipated that VS-guided lead compound discovery will regularly employ a combination of monoamine transporter and receptor targets.

In summary, virtual screening of the vestibular (S2) binding site of a LeuT-guided DAT computational model provided hMAT inhibitor MI-17 ((\pm)-1), possessing modest binding affinity for hDAT, hSERT, and hNET. Subsequent computational chemistry

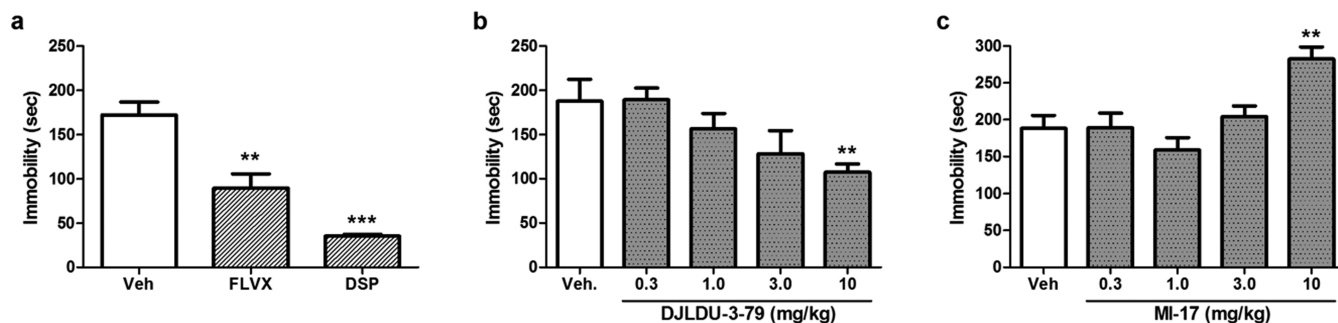


Figure 4. Behavioral effects of MI-17 ((\pm)-1) and DJLDU-3-79 ((\pm)-3) in the tail suspension test. (a) Acute administration (30 min) of the selective reuptake inhibitors of serotonin, fluvoxamine (FLVX; 10 mg/kg, i.p.), and norepinephrine, desipramine (DSP; 3 mg/kg, i.p.), decreased immobility times compared to water vehicle-treated (Veh) control animals ($n = 7$ –9). (b) DJLDU-3-79 dose-dependently decreased immobility times compared to DMSO (100%; 0.002 mL/g) vehicle-treated (Veh) animals, indicating antidepressant-like effects ($n = 8$ –14). (c) In contrast, MI-17 dose-dependently increased immobility times compared to DMSO (2%; 0.01 mL/g) vehicle-treated (Veh) animals ($n = 8$ –10). Data are presented as the mean \pm SEM and were analyzed by one-way ANOVA with Tukey's posthoc test with ** $P < 0.01$, *** $P < 0.001$ vs the appropriate vehicle control.

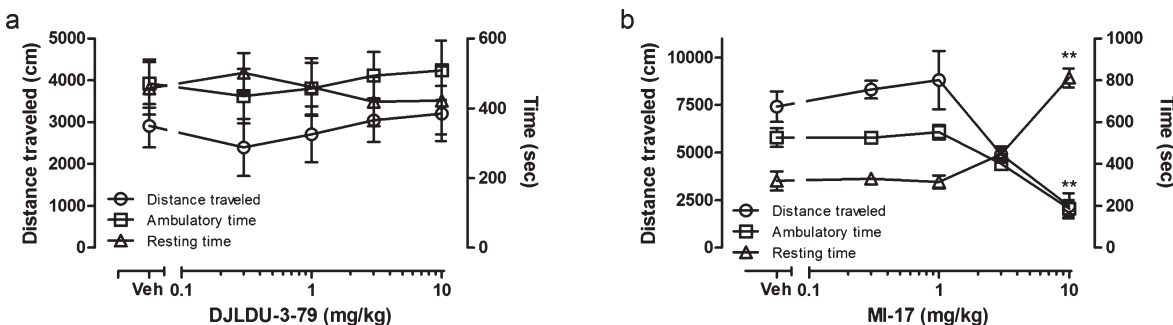


Figure 5. Locomotor effects of DJLDU-3-79 ((\pm)-3) and MI-17 ((\pm)-1). Locomotor activity was measured in animals 30 min following administration of (a) DJLDU-3-79 or (b) MI-17 and the appropriate DMSO vehicle: 100% at 0.002 mL/g or 2% at 0.01 mL/g, respectively. Behavioral responses were measured as the distance traveled (centimeters) and ambulatory time and resting time (seconds). Data are presented as the mean \pm SEM ($n = 6$ –10), and were analyzed by one-way ANOVA with Tukey's posthoc test with ** $P < 0.01$ vs vehicle-treated (Veh) control.

efforts and structural comparison of this VS hit to known SERT ligands led to the rational design and synthesis of a molecular hybrid with improved in vitro and in vivo hSERT pharmacological properties. This work highlights the utility of transporter-based virtual screening as a tool for identifying novel MAT inhibitor chemotypes and chemical fragments that may be coupled with traditional medicinal chemistry, toward developing clinical candidates for a host of CNS-based disorders.

METHODS

Materials. [³H]-WIN 35,428, [³H]-dopamine, [³H]-serotonin, [³H]-norepinephrine, and [¹²⁵I]-RTI-55 were purchased from PerkinElmer (Foster City, CA). (\pm)-1 was purchased from Enamine (Kiev, Ukraine). The N2A-hDAT cell line was a gift from Dr. Margaret Gney. HEK293 cells stably transfected with hNET or hSERT were prepared in collaboration with Dr. Mads Larsen and Dr. Susan Amara (University of Pittsburgh, Pittsburgh, PA).

Molecular Modeling. DAT Virtual Screening. Generation of the DAT homology model used in the virtual screening has been previously described.²⁰ Virtual screening was carried out in MOE as previously described,³⁴ with the exception that the entire Enamine virtual screening collection was curated and employed. An account was created at the Enamine Web site (<http://www.enamine.net/>). High-throughput screening virtual libraries 1 to 6 and Advanced Collections 1 and 2 were downloaded as SDF files. Compounds were subjected to a “wash” procedure that took into account removal of counterions and salts,

addition of explicit hydrogen atoms, and rebalancing of protonation states by deprotonating strong acids and/or protonating strong bases at pH 7. The most feasible tautomer for each compound was retained as guided by the MOE software in-house “rules”. Compounds with unconstrained chiral centers were removed from the databases (to ensure chiral purity) as well as compounds with reactive, mutagenic, and/or carcinogenic functional groups⁵⁸ beyond what is stipulated by Lipinski's Rule of Five. These operations were performed using the *sdfilter* and *sdwash.svl* commands within MOE. Finally, the SDF files with 2D coordinates were imported into a MOE molecular database, partial charges were added, and energy minimized using the Merck molecular force field MMFF94x with a conjugated gradient/truncated Newton optimization algorithm (convergence criterion = 0.05 kcal/mol, $\epsilon = 1$). These druglike, nonreactive, and enantiomerically pure databases containing one low energy conformation for each compound were employed in the docking experiments. The chemical structures and Affinity dG values for compounds MI-11 through MI-20 can be found in the Supporting Information (Figure A).

Flexible Alignment of Ligands. Flexible alignment of (\pm)-1 and 2 was performed using a stochastic conformational method in which the conformational space of each ligand is assessed while simultaneously exploring the alignment space of the compounds. Partial charges were calculated using MMFF94x prior to the conformational search. The unconstrained stereogenic center of (\pm)-1 was free to invert, affording both (*R*)- and (*S*)-enantiomers. For the alignment, an iteration limit = 200, a failure limit = 20, and the default atom-based similarity terms were used. A score was assigned to each alignment based on the average strain

energy and a similarity measure that considers molecular feature overlap. An energy cutoff = 15 kcal/mol and an rmsd tolerance for heavy atoms = 0.5 Å were set in order to retain only low energy alignments sufficiently distinct from previously generated alignments. Six alignments were generated ranging in score from -68.277 to -59.613; lower values indicate a better alignment.

SERT Modeling. The primary sequence of hSERT was downloaded from the Uniprot database (P31645) and along with LeuT_{Aa} (2a65) loaded into Discovery Studio (DS) 2.5.1.⁵⁹ The sequence alignment described by Celik et al.⁶⁰ was employed with minor modifications (Figure B in the Supporting Information). Manual modifications included movement of the gaps in the TM3 and EL2 loop region, in EL2 loop, in beta strand 2, and in TM7. These modifications increased overall sequence identity and produced a more favorable phi-psi plot. Models were generated using several different alignments, and the Figure B alignment was found to produce the best hSERT model. This model varied relative to the Beuming et al.¹⁶ alignment principally in terms of EL4, which is thought to be important to the S2 binding site. Specifically, EL4 of the Beuming-based model projected into the S2 site, hindering ligand occupancy. The “build homology” protocol available in DS was used to construct 20 models of hSERT. Based on the lowest discrete optimized potential energy (DOPE) score generated by DS, which evaluates the relative stability of a model by comparing it to other generated models, five models were picked for further refinement. The stereochemical quality of these models was evaluated using the PDB validation server. From this analysis, two of the five models were evaluated further for their fitness in a 3-D environment by using the “verify protein” (Profiles-3D) protocol. The Profiles-3D score calculated for a model should be close to the high score generated, indicating that the model has a reasonable fold. The chosen model had a score comparable to the high score and good spatial overlap with LeuT_{Aa}. Following the addition of hydrogen atoms and partial charges to the model, hydrogen atoms were minimized, keeping heavy atoms fixed to remove unwanted steric effects.

SERT Docking. Conformations were enumerated for each compound using a stochastic method followed by docking into the hSERT vestibular pocket using MOE. A wall constraint (radius = 7 Å) encompassing alpha spheres placed by the MOE Site-Finder tool was used to define the site for docking. Docking into the hSERT model was carried out using the Proxy Triangle placement method and a force field refinement. Docking poses were scored using the Affinity dG scoring method of MOE.

In Vitro MAT Binding Screen of VS “Hit” Compounds. Compounds identified from the virtual screening were dissolved in 100% DMSO to a concentration of 10 mM, and an initial one-point competition binding assay was conducted at 10 µM final concentration. Competition binding was performed using stably transfected N2A-hDAT and HEK293-hNET whole cells with [³H]-WIN 35,428 and [¹²⁵I]-RTI-55, respectively, while hSERT binding was examined using stably transfected HEK293-hSERT membrane (described below) with [¹²⁵I]-RTI-55. Nonspecific radioligand binding was determined using 10 µM concentrations of mazindol, desipramine, and paroxetine for hDAT, hNET, and hSERT, respectively. Screening results were analyzed with one-way ANOVA ($P < 0.05$) with a posthoc Dunnett’s multiple comparison test.

hNET and hDAT Whole Cell Pharmacology. Compounds were evaluated using in vitro radioligand binding assays at all three transporters. Nonspecific radioligand binding was determined using mazindol, desipramine, and paroxetine for hDAT, hNET, and hSERT, respectively. Whole-cell competition binding assays were performed for hDAT and hNET using stable N2A-hDAT or HEK293-hNET cell lines grown at 37 °C in a 5% CO₂ environment. Cell monolayers were grown in 24-well plates to >90% confluence. Cells were washed twice with 1 mL of KRH buffer (25 mM HEPES, pH 7.3, 125 mM NaCl, 4.8 mM KCl,

1.3 mM CaCl₂, 1.2 mM MgSO₄, 1.2 mM KH₂PO₄, 5.6 mM glucose) supplemented with 50 µM ascorbic acid (KRH/AA). Cells were incubated for 15 min at room temperature with 1 nM [³H]-WIN 35,428 for hDAT or 1 nM [¹²⁵I]-RTI-55 for hNET supplemented with tropolone along with increasing concentrations of drug or 10 µM mazindol (hDAT) or 10 µM desipramine (hNET) (total volume of 500 µL). Following incubation, cells were washed twice with 1 mL of KRH/AA buffer and then treated with 1 mL of 1% SDS with gentle shaking at room temperature for 1 h. Cell lysates were transferred into 5 mL of scintillation fluid for radioactivity analysis using a liquid scintillation analyzer. For saturation binding assays, data were analyzed with GraphPad Prism 5.0 software. IC₅₀ values were generated and converted to K_i values using the Cheng-Prusoff equation ($K_i = IC_{50}/(1 + ([RTI-55]/K_d RTI-55))$).

hSERT Membrane Pharmacology. hSERT binding affinities were obtained by displacement of [¹²⁵I]-RTI-55 in membrane binding assays. Membranes were prepared from stable HEK293-hSERT cells grown at 37 °C in a 5% CO₂ environment on 150 × 25 mm plates. At 95% confluence (3 days of growth), cells were washed twice with 10 mL of cold phosphate-buffered saline (DPBS). An additional 10 mL of DPBS was added, and cells were harvested by scraping and transferred to cold centrifuge tubes (15 mL), followed by centrifuging for 10 min at low speed (700g). After removal of the supernatant, the cell pellet was resuspended in 500 µL of cold TE buffer (50 mM Tris, 1 mM EDTA, pH 7.5). Following centrifuging for 30 min at 100 000g at 4 °C, the supernatant was discarded and the pellet was frozen for later use or resuspended in ice-cold binding buffer (50 mM Tris, pH 7.5, 100 mM NaCl). Each sample was analyzed for protein content using the Bradford protein assay. For competition binding, membranes were incubated at room temperature with [¹²⁵I]-RTI-55 (0.1 nM concentration) and increasing concentrations of cold competitor (1 fM to 1 µM) or 10 µM paroxetine to measure nonspecific binding. Reactions were carried out in 12 × 75 mm borosilicate glass tubes with gentle shaking at room temperature for 1 h and terminated by rapid filtration through GF/B filters (Schleicher and Schuell, Keene, NH) presoaked in 0.5% polyethylenimine solution (v/v). Filters were washed twice with 5 mL of cold 50 mM Tris buffer and transferred to vials. Radioactivity was determined using a Beckman gamma counter. Data were analyzed with GraphPad Prism 5.0 software. IC₅₀ values were generated and converted to K_i values using the Cheng-Prusoff equation ($K_i = IC_{50}/(1 + ([RTI-55]/K_d RTI-55))$).

Substrate Uptake Inhibition Assays. A substrate uptake inhibition screening assay was performed in parallel with the one-point competition-binding assay. Stably transfected N2A-hDAT, HEK293-hNET, and HEK293-hSERT cells were grown to >90% confluence on 24-well plates. Cells were washed and then preincubated with inhibitor (10 µM) for 10 min at room temperature, followed by addition of 10 nM [³H]-dopamine, [³H]-norepinephrine, or [³H]-serotonin. After 5 min, cells were washed twice then treated with 5% SDS and shaken for 1 h. Lysates were transferred to 5 mL of scintillation fluid, and radioactivity was detected using a liquid scintillation analyzer. Nonspecific radioligand binding was determined using 10 µM concentrations of mazindol, desipramine, and paroxetine for hDAT, hNET, and hSERT, respectively. VS compounds demonstrating the ability to decrease net uptake of [³H]-neurotransmitter in the screening assay were characterized further using a range of concentrations, typically 0.01–10 000 nM, to determine IC₅₀ values (GraphPad Prism 5, La Jolla, CA).

General Experimental Approach for Organic Synthesis. Reaction conditions and yields were not optimized. All reactions were performed in flame-dried glassware under argon unless otherwise noted. All solvents and chemicals were purchased from Aldrich Chemical Co. or Fisher Scientific and used without further purification. Flash column chromatography was performed according to the method of Still et al.⁶¹ using Fisher S826-25 silica gel sorbent (70–230 mesh) and eluting

solvent mixtures as specified. Thin-layer chromatography (TLC) was performed using TLC silica gel 60 F₂₅₄ plates obtained from EMD Chemicals, Inc., and compounds were visualized under UV light and/or I₂ stain. Proportions of solvents used for TLC are by volume. ¹H and ¹³C NMR spectra were recorded on either a Bruker 400 or 500 MHz spectrometer. Chemical shifts for ¹H and ¹³C NMR spectra are reported as parts per million (δ ppm) relative to tetramethylsilane (0.00 ppm) as an internal standard. Coupling constants are measured in Hz. HRMS samples were analyzed at Old Dominion University (Norfolk, VA) by positive ion electrospray on a Bruker 12 T APEX -Qe FTICR-MS instrument with an Apollo II ion source. On the basis of ¹H and ¹³C NMR, all compounds were >95% pure.

Synthesis of Molecular Hybrid (±)-DJLDU-3-79 ((±)-3). A suspension of 2-chlorobenzyl alcohol (1.4 g, 10 mmol, Aldrich), *n*-Bu₄NBr (160 mg, 0.5 mmol, Acros), and 40% (w/v) aq. NaOH solution (13 mL) was initially stirred at room temperature and then cooled to 0 °C. Racemic epichlorohydrin (3.1 mL, 40 mmol, Aldrich) was then added dropwise via syringe. The resulting mixture was stirred at 0 °C for 30 min, then the ice bath was removed, and the reaction was allowed to stir at room temperature overnight. After 18 h, the mixture was poured onto ice with the aid of H₂O and Et₂O, and then extracted. The organic layer was dried (MgSO₄), filtered, and concentrated to provide 1.91 g (97% yield) of benzyl ether (±)-4 as a light brown oil. ¹H NMR indicated the material was sufficiently pure to take directly on to the next reaction without further purification. Characterization data for (±)-4: R_f = 0.42 (EtOAc/hexanes, 2:8). ¹H NMR (CDCl₃, 400 MHz): δ 7.50 (dd, 1H, J = 2 Hz, 7.6 Hz), 7.35 (dd, 1H, J = 1.6 Hz, 7.6 Hz), 7.29–7.21 (m, 2H), 4.68 (q, 2H, J = 12.8 Hz), 3.85 (dd, 1H, J = 3.2 Hz, 11.2 Hz), 3.52 (dd, 1H, J = 6 Hz, 12 Hz), 3.23 (m, 1H), 2.83 (dd, 1H, J = 4.8 Hz, 4 Hz), 2.66 (dd, 1H, J = 2.8 Hz, 4.8 Hz). ¹³C NMR (CDCl₃, 100 MHz): δ 135.7, 132.9, 129.3, 129.1, 128.8, 126.8, 71.4, 70.3, 50.8, 44.3. HRMS calculated for (C₁₀H₁₁ClO₂)^{2Na⁺} 419.0787, found 419.0794. A solution of tetrahydropyridine 5⁴³ (589 mg, 3 mmol) and epoxide (±)-4 (393 mg, 2 mmol) in DMSO (14 mL) was heated at 77 °C for 5 h. During the course of the reaction, the mixture changed from a yellow to orange solution. After cooling to room temperature, the mixture was poured into H₂O then extracted with EtOAc. The organic layer was washed with brine, dried (MgSO₄), filtered, concentrated, and chromatographed (95:3:2, CHCl₃/MeOH/Et₃N) to provide 750 mg (95%) of (±)-3 as a brown oil. Characterization data for (±)-3: R_f = 0.36 (CHCl₃: MeOH, 9:1). ¹H NMR (CDCl₃, 400 MHz): δ 8.32 (br s, 1H), 7.88 (d, 1H, J = 8.4 Hz), 7.51 (dd, 1H, J = 2.0 Hz, 7.6 Hz), 7.38–7.34 (m, 2H), 7.29–7.12 (m, 5H), 6.19 (t, 1H, J = 3.2 Hz), 4.69 (s, 2H), 4.07 (m, 1H), 3.62 (qd, 2H, J = 4.4 Hz, 11.6 Hz), 3.40 (dd, 1H, J = 3.2 Hz, 16.4 Hz), 3.22 (dd, 1H, J = 3.2 Hz, 16.4 Hz), 2.92 (m, 1H), 2.73 (m, 1H), 2.68–2.56 (m, 5H). ¹³C NMR (CDCl₃, 100 MHz): δ 136.8, 135.9, 133.0, 129.8, 129.3, 129.2, 128.7, 126.8, 125.1, 122.2, 121.4, 120.6, 120.1, 118.8, 117.7, 111.4, 73.3, 70.5, 66.5, 60.5, 53.2, 41.0, 28.9. HRMS calculated for (C₂₃H₂₅Cl₁N₂O₂)^{2H⁺} 397.1677, found 397.1682.

Behavioral Conditions. At weaning, male C57BL/6J mice were group housed (six animals per cage) with same-sex littermates, in a temperature- and humidity-controlled vivarium, under a 12 h light/dark cycle (lights on at 7:00 a.m.). Behavioral testing was conducted during the light phase of the light/dark cycle between 9:00 a.m. and 12:00 pm. Animals used in behavioral studies were typically between 10 and 24 weeks of age and were naive to all behavioral treatments prior to testing. Room luminance was maintained between 70 and 75 foot candles for all behavioral studies. Unless specified otherwise, drugs were administered intraperitoneally (i.p.) 30 min prior to behavioral testing. Sterile water was the vehicle used with fluvoxamine and desipramine; the vehicle DMSO at 2% (0.01 mL/g) or 100% (0.002 mL/g) was employed with MI-17 or DJLDU-3-79, respectively. All experimental procedures were approved by the local Institutional Animal Care and Use Committee and

followed the National Institute of Health guidelines outlined in "Using Animals in Intramural Research".

Mouse Tail Suspension Test. As previously described,⁶² mice were individually suspended by the tail from a metal bar elevated 30 cm using adhesive tape. Behavior was videotaped for 6 min and videos were later scored for immobility time (seconds) by a blinded observer.

Locomotor Activity. Locomotor activity was assessed as described⁶² in a noninvasive manner using a Opto-Varimax 4 activity analyzer (Columbus Instruments, Columbus, OH) that measures animal activity in a cage intersected with photocells projecting infrared beams 2.5 cm apart and 2 cm above the floor. After a brief habituation period, animals were treated with either drug or the appropriate vehicle and activity was measured for 20 min.

ASSOCIATED CONTENT

Supporting Information. Figure A: Virtual screening hits MI-11 through MI-20. The Affinity dG docking score is indicated below each structure in the figure. Figure B: LeuT–hSERT polypeptide sequence alignment used in the generation of the hSERT model. This material is available free of charge via the Internet at <http://pubs.acs.org>.

AUTHOR INFORMATION

Corresponding Author

(D.J.L.) Mailing address: Division of Pharmaceutical Sciences, Mylan School of Pharmacy, Duquesne University, 422B Mellon Hall, 600 Forbes Avenue, Pittsburgh, PA 15282. E-mail: lapinskyd@duq.edu. **(J.D.M.)** Mailing address: Departments of Chemistry and Biochemistry, Duquesne University, 312 Mellon Hall, 600 Forbes Avenue, Pittsburgh, PA 15282. E-mail: madura@duq.edu **(C.K.S.)** Mailing address: Division of Pharmaceutical Sciences, Mylan School of Pharmacy, Duquesne University, 411 Mellon Hall, 600 Forbes Avenue, Pittsburgh, PA 15282. E-mail: surratt@duq.edu.

Author Contributions

T.L.N. conducted SERT and NET pharmacological assays, performed molecular modeling studies, and wrote the first draft of the manuscript. D.J.L. devised the molecular hybridization strategy, carried out all organic synthesis, and wrote portions of the manuscript. J.N.T. wrote a portion of the manuscript and designed and oversaw all animal studies; L.M.G., M.E.A., and P.N.T. collaborated on these studies. M.I. carried out ligand virtual screening using the DAT computational model he generated (reported in ref 20) to provide the compounds MI-10 through MI-20. Y.L. conducted initial DAT and SERT pharmacologic screening of VS hits, DAT pharmacology of DJLDU-3-79, and SERT pharmacology of MI-17. S.M. created the SERT molecular model and contributed to manuscript writing. J.D.M. oversaw and contributed to the computational model building and contributed to the manuscript. C.K.S. launched the efforts to create the computational models, guided and consulted on pharmacologic assays and data interpretation, and wrote portions of the manuscript.

Funding Sources

This work was supported by NIDA Grants DA026530 (to C.K.S.) and DA027806 (to J.D.M.), Department of Education equipment Grants P116Z050331 and P116Z080180 (to J.D.M.), and the Bower, Bennett, and Bennett Endowed Chair Research Award (to J.N.T.), and by a Duquesne University Faculty Development Fund grant (to D.J.L.).

■ ACKNOWLEDGMENT

We thank Drs. Mads Larsen and Susan Amara for collaboration in preparing the hSERT and hNET HEK cell lines. M.I. would like to thank Drs. Jack Smith and Jaime Hargrave (University of Texas—Houston, School of Biomedical Informatics) for fellowship support.

■ ABBREVIATIONS

MAT, monoamine transporter protein; hDAT, plasma membrane human dopamine transporter protein; hSERT, plasma membrane human serotonin transporter protein; hNET, plasma membrane human norepinephrine transporter protein; SSRI, selective serotonin reuptake inhibitor; VS, virtual screening; TST, tail suspension test

■ REFERENCES

- (1) Amara, S., and Sonders, M. S. (1998) Neurotransmitter transporters as molecular targets for addictive drugs. *Drug Alcohol Depend.* **51**, 87–96.
- (2) Hahn, M. K., Robertson, D., and Blakely, R. D. (2003) A mutation in the human norepinephrine transporter gene (SLC6A2) associated with orthostatic intolerance disrupts surface expression of mutant and wild-type transporters. *J. Neurosci.* **23**, 4470–4478.
- (3) Bowton, E., Saunders, C., Erreger, K., Sakrikar, D., Matthies, H. J., Sen, N., Jessen, T., Colbran, R. J., Caron, M. G., Javitch, J. A., Blakely, R. D., and Galli, A. (2010) Dysregulation of dopamine transporters via dopamine D2 autoreceptors triggers anomalous dopamine efflux associated with attention-deficit hyperactivity disorder. *J. Neurosci.* **30**, 6048–6057.
- (4) Wong, D. F., Harris, J. C., Naidu, S., Yokoi, F., Marenco, S., Dannals, R. F., Ravert, H. T., Yaster, M., Evans, A., Rousset, O., Bryan, R. N., Gjedde, A., Kuhar, M. J., and Breese, G. R. (1996) Dopamine transporters are markedly reduced in Lesch-Nyhan disease *in vivo*. *Proc. Natl. Acad. Sci. U.S.A.* **93**, 5539–5543.
- (5) Prasad, H. C., Steiner, J. A., Sutcliffe, J. S., and Blakely, R. D. (2009) Enhanced activity of human serotonin transporter variants associated with autism. *Philos. Trans. R. Soc. London Biol. Sci.* **364**, 163–173.
- (6) Hahn, M. K., and Blakely, R. D. (2002) Monoamine transporter gene structure and polymorphisms in relation to psychiatric and other complex disorders. *Pharmacogenomics J.* **2**, 217–235.
- (7) Ramamoorthy, S., Bauman, A. L., Moore, K. R., Han, H., Yang-Feng, T., Chang, A. S., Ganapathy, V., and Blakely, R. D. (1993) Antidepressant- and cocaine-sensitive human serotonin transporter” Molecular cloning, expression, and chromosomal localization. *Proc. Natl. Acad. Sci. U.S.A.* **90**, 2542–2546.
- (8) Ozaki, N., Goldman, D., Kaye, W. H., Greenberg, B. D., Lappalainen, J., Rudnick, G., and Murphy, D. L. (2003) Serotonin transporter missense mutation associated with a complex neuropsychiatric phenotype. *Mol. Psychiatry* **8**, 933–936.
- (9) Ferguson, J. M. (2001) SSRI antidepressant medications: Adverse effects and tolerability. *Prim. Care Compan. J. Clin. Psychiatry* **3**, 22–27.
- (10) Kennedy, S. H., Andersen, H. F., and Lam, R. W. (2006) Efficacy of escitalopram in the treatment of major depressive disorder compared with conventional selective serotonin reuptake inhibitors and venlafaxine XR: a meta-analysis. *J. Psychiatry Neurosci.* **31**, 122–131.
- (11) Preskorn, S. H. (1995) Comparison of the tolerability of bupropion, fluoxetine, imipramine, nefazodone, paroxetine, sertraline, and venlafaxine. *J. Clin. Psychiatry* **56** (Suppl 6), 12–21.
- (12) Schellander, R., and Donnerer, J. (2010) Antidepressants: Clinically relevant drug interactions to be considered. *Pharmacology* **86**, 203–215.
- (13) Gu, H., Wall, S. C., and Rudnick, G. (1994) Stable expression of biogenic amine transporters reveals differences in inhibitor sensitivity, kinetics, and ion dependence. *J. Biol. Chem.* **269**, 7124–7130.
- (14) McElvain, J. S., and Schenk, J. O. (1992) A multisubstrate mechanism of striatal dopamine uptake and its inhibition by cocaine. *Biochem. Pharmacol.* **43**, 2189–2199.
- (15) Rudnick, G. (2002) In *Neurotransmitter Transporters, Structure, Function, and Regulation* (Reith, M. E. A., Ed.), 2nd ed., pp 25–52, Humana Press, Totowa, NJ.
- (16) Beuming, T., Shi, L., Javitch, J. A., and Weinstein, H. (2006) A comprehensive structure-based alignment of prokaryotic and eukaryotic neurotransmitter/Na⁺ symporters (NSS) aids in the use of the LeuT structure to probe NSS structure and function. *Mol. Pharmacol.* **70**, 1630–1642.
- (17) Yamashita, A., Singh, S. K., Kawate, T., Jin, Y., and Gouaux, E. (2005) Crystal structure of a bacterial homologue of Na⁺/Cl⁻-dependent neurotransmitter transporters. *Nature* **437**, 215–223.
- (18) Andersen, J., Olsen, L., Hansen, K. B., Taboureaux, O., Jorgensen, F. S., Jorgensen, A. M., Bang-Andersen, B., Egebjerg, J., Stromgaard, K., and Kristensen, A. S. (2009) Mutational mapping and modeling of the binding site for (S)-citalopram in the human serotonin transporter. *J. Biol. Chem.* **285**, 2051–2063.
- (19) Forrest, L. R., Zhang, Y. W., Jacobs, M. T., Gesmonde, J., Xie, L., Honig, B. H., and Rudnick, G. (2008) Mechanism for alternating access in neurotransmitter transporters. *Proc. Natl. Acad. Sci. U.S.A.* **105**, 10338–10343.
- (20) Indarte, M., Madura, J. D., and Surratt, C. K. (2008) Dopamine transporter comparative molecular modeling and binding site prediction using the LeuTAa leucine transporter as a template. *Proteins* **70**, 1033–1046.
- (21) Sarker, S., Weissensteiner, R., Steiner, I., Sitte, H. H., Ecker, G. F., Freissmuth, M., and Sucic, S. (2010) The high-affinity binding site for tricyclic antidepressants resides in the outer vestibule of the serotonin transporter. *Mol. Pharmacol.* **78**, 1026–1035.
- (22) Beuming, T., Kniazeff, J., Bergmann, M. L., Shi, L., Gracia, L., Raniszewska, K., Newman, A. H., Javitch, J. A., Weinstein, H., Gether, U., and Loland, C. J. (2008) The binding sites for cocaine and dopamine in the dopamine transporter overlap. *Nat. Neurosci.* **11**, 780–789.
- (23) Boudker, O., and Verdon, G. (2010) Structural perspectives on secondary active transporters. *Trends Pharmacol. Sci.* **31**, 418–426.
- (24) Shi, L., Quick, M., Zhao, Y., Weinstein, H., and Javitch, J. A. (2008) The mechanism of a neurotransmitter:sodium symporter—inward release of Na⁺ and substrate is triggered by substrate in a second binding site. *Mol. Cell* **30**, 667–677.
- (25) Zhao, Y., Terry, D. S., Shi, L., Quick, M., Weinstein, H., Blanchard, S. C., and Javitch, J. A. (2011) Substrate-modulated gating dynamics in a Na⁽⁺⁾-coupled neurotransmitter transporter homologue. *Nature* **474**, 109–113.
- (26) Sinning, S., Musgaard, M., Jensen, M., Severinsen, K., Celik, L., Koldsoe, H., Meyer, T., Bols, M., Jensen, H. H., Schiott, B., and Wiborg, O. (2010) Binding and orientation of tricyclic antidepressants within the central substrate site of the human serotonin transporter. *J. Biol. Chem.* **285**, 8363–8374.
- (27) Thompson, B. J., Jessen, T., Henry, L. K., Field, J. R., Gamble, K. L., Gresch, P. J., Carneiro, A. M., Horton, R. E., Chisnell, P. J., Belova, Y., McMahon, D. G., Daws, L. C., and Blakely, R. D. (2011) Transgenic elimination of high-affinity antidepressant and cocaine sensitivity in the presynaptic serotonin transporter. *Proc. Natl. Acad. Sci. U.S.A.* **108**, 3785–3790.
- (28) Singh, S. K., Yamashita, A., and Gouaux, E. (2007) Antidepressant binding site in a bacterial homologue of neurotransmitter transporters. *Nature* **448**, 952–956.
- (29) Zhou, Z., Zhen, J., Karpowich, N. K., Goetz, R. M., Law, C. J., Reith, M. E. A., and Wang, D. N. (2007) LeuT-desipramine structure reveals how antidepressants block neurotransmitter reuptake. *Science* **317**, 1390–1393.
- (30) Zhou, Z., Zhen, J., Karpowich, N. K., Law, C. J., Reith, M. E. A., and Wang, D.-N. (2009) Antidepressant specificity of serotonin transporter suggested by three LeuT–SSRI structures. *Nat. Struct. Mol. Biol.* **16**, 652–657.
- (31) Andersen, J., Taboureaux, O., Hansen, K. B., Olsen, L., Egebjerg, J., Stromgaard, K., and Kristensen, A. S. (2009) Location of the antidepressant binding site in the serotonin transporter: Importance

- of Ser-438 in recognition of citalopram and tricyclic antidepressants. *J. Biol. Chem.* 284, 10276–10284.
- (32) Bailey, D., and Brown, D. (2001) High-throughput chemistry and structure-based design: survival of the smartest. *Drug Discovery Today* 6, S7–S9.
- (33) Schneider, G., and Bohm, H. J. (2002) Virtual screening and fast automated docking methods. *Drug Discovery Today* 7, 64–70.
- (34) Indarte, M., Liu, Y., Madura, J. D., and Surratt, C. K. (2010) Receptor-based discovery of a plasmalemmal monoamine transporter inhibitor via high-throughput docking and pharmacophore modeling. *ACS Chem. Neurosci.* 1, 223–233.
- (35) (2010) Molecular Operating Environment (MOE), In 2010.10, Chemical Computing Group Inc., Montreal, QC, Canada.
- (36) Butler, S. G., and Meegan, M. J. (2008) Recent developments in the design of anti-depressive therapies: targeting the serotonin transporter. *Curr. Med. Chem.* 15, 1737–1761.
- (37) Zhou, D., Stack, G. P., Lo, J., Failli, A. A., Evrard, D. A., Harrison, B. L., Hatzenbuhler, N. T., Tran, M., Croce, S., Yi, S., Golembieski, J., Hornby, G. A., Lai, M., Lin, Q., Schecter, L. E., Smith, D. L., Shilling, A. D., Huselton, C., Mitchell, P., Beyer, C., and Andree, T. H. (2009) Synthesis, potency, and in vivo evaluation of 2-piperazin-1-ylquinoline analogues as dual serotonin reuptake inhibitors and serotonin 5-HT1A receptor antagonists. *J. Med. Chem.* 52, 4955–4959.
- (38) Herold, F., Chodkowski, A., Izbicki, L., Turlo, J., Dawidowski, M., Kleps, J., Nowak, G., Stachowicz, K., Dybala, M., Siwek, A., Mazurek, A. P., Mazurek, A., and Plucinski, F. (2011) Novel 4-aryl-pyrido[1,2-c]pyrimidines with dual SSRI and 5-HT(1A) activity. part 3. *Eur. J. Med. Chem.* 46, 142–149.
- (39) Herold, F., Izbicki, Ł., Chodkowski, A., Dawidowski, M., Król, M., Kleps, J., Turło, J., Wolska, I., Nowak, G., and Stachowicz, K. (2009) Novel 4-aryl-pyrido[1,2-c]pyrimidines with dual SSRI and 5-HT1A activity: Part 2. *Eur. J. Med. Chem.* 44, 4702–4715.
- (40) Tomlinson, I. D., Iwamoto, H., Blakely, R. D., and Rosenthal, S. J. (2011) Biotin tethered homotryptamine derivatives: high affinity probes of the human serotonin transporter (hSERT). *Bioorg. Med. Chem. Lett.* 21, 1678–1682.
- (41) Viegas-Junior, C., Danuello, A., da Silva Bolzani, V., Barreiro, E. J., and Fraga, C. A. M. (2007) Molecular hybridization: A useful tool in the design of new drug prototypes. *Curr. Med. Chem.* 14, 1829–1852.
- (42) Sun, F., Xu, G., Wu, J., and Yang, L. (2006) Efficient lipase-catalyzed kinetic resolution of 4-arylmethoxy-3-hydroxybutanenitriles: Application to an expedient synthesis of a statin intermediate. *Tetrahedron: Asymmetry* 17, 2907–2913.
- (43) Foquerana, S., Miralpeix, M., Pages, L., Puig, C., Cardus, A., Anton, F., Cardenas, A., Vilella, D., Aparici, M., Calaf, E., Prieto, J., Gras, J., Huerta, J. M., Warrelow, G., Beleta, J., and Ryder, H. (2004) Synthesis and structure-activity relationships of novel histamine H1 antagonists: Indolylperidinyl benzoic acid derivatives. *J. Med. Chem.* 47, 6326–6337.
- (44) Chan, A. W., Curran, T. T., Iera, S., Sellstedt, J. H., Vid, G., Feigelson, G., Ding, Z. (2002) Processes for the synthesis of derivatives of 2,3-dihydro-1,4-dioxino-[2,3-f] quinoline, U.S. Patent WO/2002/092602.
- (45) Cryan, J. F., and Holmes, A. (2005) The ascent of mouse: advances in modeling human depression and anxiety. *Nat. Rev. Drug Discovery* 4, 775–790.
- (46) Steru, L., Chermat, R., Thierry, B., and Simon, P. (1985) The tail suspension test: a new method for screening antidepressants in mice. *Psychopharmacology (Heidelberg, Ger.)* 85, 367–370.
- (47) Kim, C. Y., Mahaney, P. E., McConnell, O., Zhang, Y., Manas, E., Ho, D. M., Deecher, D. C., and Trybulski, E. J. (2009) Discovery of a new series of monoamine reuptake inhibitors, the 1-amino-3-(1H-indol-1-yl)-3-phenylpropan-2-ols. *Bioorg. Med. Chem. Lett.* 19, 5029–5032.
- (48) O'Neill, D. J., Adedoyin, A., Alfinito, P. D., Bray, J. A., Cosmi, S., Deecher, D. C., Fensome, A., Harrison, J., Leventhal, L., Mann, C., McComas, C. C., Sullivan, N. R., Spangler, T. B., Uveges, A. J., Trybulski, E. J., Whiteside, G. T., and Zhang, P. (2010) Discovery of novel selective norepinephrine reuptake inhibitors: 4-[3-aryl-2,2-dioxido-2,1,3-benzothiadiazol-1(3H)-yl]-1-(methylamino)butan-2-ols (WYE-103231). *J. Med. Chem.* 53, 4511–4521.
- (49) Tebben, A. J., and Schnur, D. M. (2011) Beyond rhodopsin: G protein-coupled receptor structure and modeling incorporating the beta2-adrenergic and adenosine alpha2A crystal structures. *Methods Mol. Biol.* 672, 359–386.
- (50) Cherezov, V., Rosenbaum, D. M., Hanson, M. A., Rasmussen, S. G., Thian, F. S., Kobilka, T. S., Choi, H. J., Kuhn, P., Weis, W. I., Kobilka, B. K., and Stevens, R. C. (2007) High-resolution crystal structure of an engineered human beta2-adrenergic G protein-coupled receptor. *Science* 318, 1258–1265.
- (51) Warne, T., Serrano-Vega, M. J., Baker, J. G., Moukhametzianov, R., Edwards, P. C., Henderson, R., Leslie, A. G., Tate, C. G., and Schertler, G. F. (2008) Structure of a beta1-adrenergic G-protein-coupled receptor. *Nature* 454, 486–491.
- (52) Chien, E. Y., Liu, W., Zhao, Q., Katritch, V., Han, G. W., Hanson, M. A., Shi, L., Newman, A. H., Javitch, J. A., Cherezov, V., and Stevens, R. C. (2010) Structure of the human dopamine D3 receptor in complex with a D2/D3 selective antagonist. *Science* 330, 1091–1095.
- (53) Ahmed, A., Choo, H., Cho, Y. S., Park, W. K., and Pae, A. N. (2009) Identification of novel serotonin 2C receptor ligands by sequential virtual screening. *Bioorg. Med. Chem.* 17, 4559–4568.
- (54) Isberg, V., Balle, T., Sander, T., Jorgensen, F. S., and Gloriam, D. E. (2011) G protein- and agonist-bound serotonin 5-HT(2A) receptor model activated by steered molecular dynamics simulations. *J. Chem. Inf. Model.* 51, 315–325.
- (55) Renault, N., Gohier, A., Chavatte, P., and Farce, A. (2010) Novel structural insights for drug design of selective 5-HT(2C) inverse agonists from a ligand-biased receptor model. *Eur. J. Med. Chem.* 45, 5086–5099.
- (56) Simpson, L. M., Wall, I. D., Blaney, F. E., and Reynolds, C. A. (2011) Modeling GPCR active state conformations: The beta(2)-adrenergic receptor. *Proteins* 79, 1441–1457.
- (57) Ivetaç, A., and McCammon, J. A. (2010) Mapping the druggable allosteric space of G-protein coupled receptors: a fragment-based molecular dynamics approach. *Chem. Biol. Drug Des.* 76, 201–217.
- (58) Kazius, J., McGuire, R., and Bursi, R. (2005) Derivation and validation of toxicophores for mutagenicity prediction. *J. Med. Chem.* 48, 312–320.
- (59) (2010) *Discovery Studio Modeling Environment*, 2.5.1 ed., Accelrys Software Inc., San Diego.
- (60) Celik, L., Sinning, S., Severinsen, K., Hansen, C. G., Moller, M. S., Bols, M., Wiborg, O., and Schiott, B. (2008) Binding of serotonin to the human serotonin transporter. Molecular modeling and experimental validation. *J. Am. Chem. Soc.* 130, 3853–3865.
- (61) Still, W. C., Kahn, M., and Mitra, A. (1978) Rapid chromatographic technique for preparative separations with moderate resolution. *J. Org. Chem.* 43, 2923–2925.
- (62) Talbot, J. N., Jutkiewicz, E. M., Graves, S. M., Clemans, C. F., Nicol, M. R., Huang, X., Mortensen, R. M., Neubig, R. R., and Traynor, J. R. (2010) RGS inhibition selectively potentiates serotonin-mediated antidepressant effects. *Proc. Natl. Acad. Sci. U.S.A.* 107, 11086–11091.
- (63) (2008) *PyMOL Molecular Graphics System*, Mac OS X ed., Schrodinger, LLC, New York.